

Rotating Wave Approximation and Rotating Frame Approximation

Symbolic Derivations and Six Numerical Worked Examples

Onri Jay Benally

December 14, 2025

Abstract

In driven two-level physics, and also in nuclear magnetic resonance and modern superconducting quantum hardware, one repeatedly rewrites a rapidly oscillating problem into a slowly evolving one. Here, we derive the rotating wave approximation (RWA) from the interaction picture and from time-averaging arguments, and then we derive the rotating frame approximation (RFA) from an explicit time-dependent unitary frame change plus a controlled removal of terms oscillating at twice the carrier. After each symbolic development, we provide three distinct worked examples with real numerical values, giving six total numerical examples. Along the way, we highlight the leading correction (the Bloch–Siegert shift), and we connect the approximations to Floquet theory and to Landau–Zener adiabatic passage.

Contents

1 Acronym glossary, symbol glossary, and short terminology notes	3
1.1 Acronym glossary	3
1.2 Symbol glossary	3
1.3 Short terminology notes, including etymological hints	3
2 Concept map	4
3 Rotating wave approximation (RWA)	5
3.1 Intuitive explanation	5
3.2 Graduate level derivation: interaction picture, frequency separation, and a controlled averaging bound	5
3.2.1 Driven two-level Hamiltonian and operator identities	5
3.2.2 Interaction picture	5
3.2.3 The approximation step, made explicit	5
3.2.4 Leading correction: Bloch–Siegert shift (linear drive)	6
3.2.5 A practical “make it exact” note	6
3.3 Three numerical RWA examples (with real values)	6
3.3.1 Example RWA-1: superconducting qubit driven at 5.000 GHz	6
3.3.2 Example RWA-2: proton NMR at 3.0 T with a weak RF field	7
3.3.3 Example RWA-3: optical transition near 384.230 THz	8
3.3.4 RWA examples summary table	8

4 Rotating frame approximation (RFA)	9
4.1 Intuitive explanation	9
4.2 Graduate level derivation: explicit rotating frame transformation, then the approximation step	9
4.2.1 Exact rotating frame transformation (RFT)	9
4.2.2 Choosing the reference rate and isolating $2\omega_d$ terms	9
4.2.3 Rotating frame approximation (RFA)	10
4.2.4 Time-dependent phase or frequency (why rotating frames keep paying off) . .	10
4.3 Three numerical rotating frame approximation examples (with real values)	10
4.3.1 Example RFA-1: resonant single-qubit X and Y gates by phase choice	10
4.3.2 Example RFA-2: off-resonant MRI-like scenario, effective field tilt in the rotating frame	11
4.3.3 Example RFA-3: chirped drive (adiabatic rapid passage) and a Landau–Zener estimate	11
4.3.4 RFA examples summary table	12
5 Context, lineage, and “where to go next”	13

1 Acronym glossary, symbol glossary, and short terminology notes

1.1 Acronym glossary

Acronym	Meaning
RWA	rotating wave approximation
RFA	rotating frame approximation
RFT	rotating frame transformation (exact change of variables/ frame)
NMR	nuclear magnetic resonance
MRI	magnetic resonance imaging
RF	radio frequency
LZ	Landau–Zener
LZS	Landau–Zener–Stückelberg
BS	Bloch–Siegert
IP	interaction picture

1.2 Symbol glossary

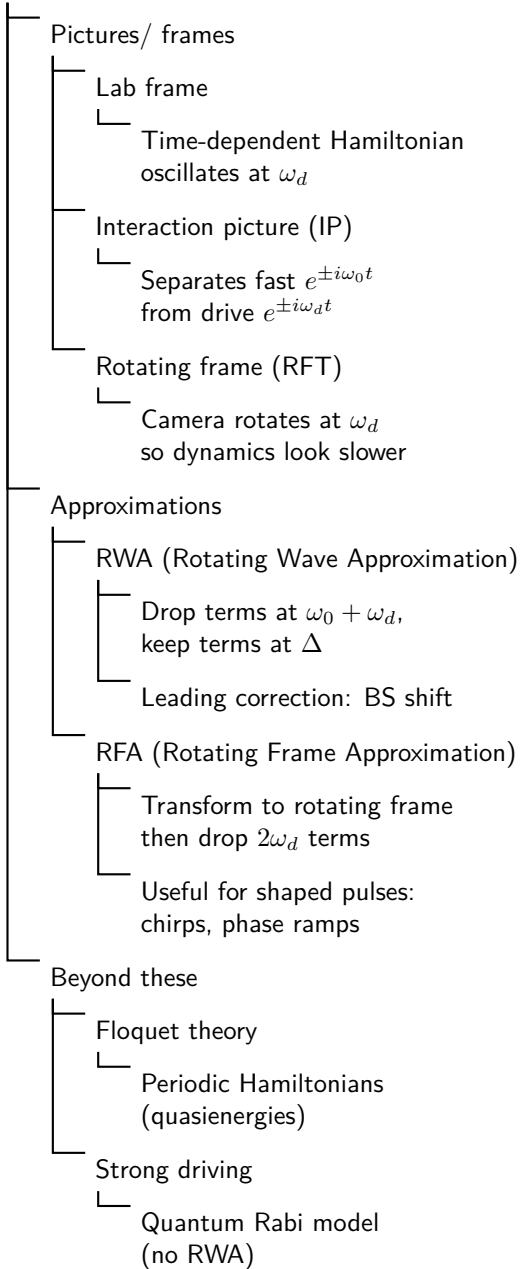
Symbol	Meaning
\hbar	reduced Planck constant
$\sigma_x, \sigma_y, \sigma_z$	Pauli operators
σ_+, σ_-	raising and lowering operators: $\sigma_+ = (\sigma_x + i\sigma_y)/2$, $\sigma_- = (\sigma_x - i\sigma_y)/2$
ω_0	bare (undriven) transition angular frequency
ω_d	drive angular frequency
Ω	drive-strength parameter, chosen so that on resonance the Rabi oscillation angular frequency is Ω under the RWA
Δ	detuning $\Delta = \omega_0 - \omega_d$
f	ordinary frequency (Hz), related by $\omega = 2\pi f$
$\ \cdot\ $	operator norm (any consistent submultiplicative norm suffices for bounds)

1.3 Short terminology notes, including etymological hints

The word *rotation* traces to Latin *rota* (wheel), while *approximation* traces to Latin *approximare* (to come near). In practice, the rotating wave approximation (RWA) comes from keeping *near-resonant* terms, and, simultaneously, from discarding *far off resonant* terms whose net effect averages toward zero over many cycles. If the discarded terms do *not* average to zero, then one can often make the approximation closer to exactness by changing the physical drive from linear polarization to circular polarization, because that change can eliminate the counter-rotating component altogether (in that special case, what is usually approximate can become exact).

2 Concept map

Driven two-level system
(rapid carrier + slow envelope)



3 Rotating wave approximation (RWA)

3.1 Intuitive explanation

When you push a playground swing, you can, effectively and repeatedly, add energy if you push in step with the swing, and you mostly fail to add energy if you push at the wrong times. In a driven two-level quantum system, the drive contains both a component that looks synchronized with the system's natural oscillation, and another component that looks like it is running “the wrong way around” at roughly twice the carrier rate. If you watch long enough, that wrong-way component pushes forward and then backward, so its net effect nearly cancels. The rotating wave approximation (RWA) is the controlled step where you keep the synchronized component and discard the canceling component.

3.2 Graduate level derivation: interaction picture, frequency separation, and a controlled averaging bound

3.2.1 Driven two-level Hamiltonian and operator identities

Consider a two-level system with a classical near-resonant drive,

$$H(t) = \frac{\hbar\omega_0}{2} \sigma_z + \hbar\Omega \cos(\omega_d t + \phi) \sigma_x. \quad (1)$$

Define the ladder operators

$$\sigma_+ \equiv \frac{\sigma_x + i\sigma_y}{2}, \quad \sigma_- \equiv \frac{\sigma_x - i\sigma_y}{2}, \quad \Rightarrow \quad \sigma_x = \sigma_+ + \sigma_-. \quad (2)$$

3.2.2 Interaction picture

Let $H_0 = \frac{\hbar\omega_0}{2}\sigma_z$ and $V(t) = \hbar\Omega \cos(\omega_d t + \phi) \sigma_x$. In the interaction picture (IP),

$$V_I(t) = e^{+iH_0 t/\hbar} V(t) e^{-iH_0 t/\hbar}. \quad (3)$$

Using $e^{+i\frac{\omega_0 t}{2}\sigma_z} \sigma_+ e^{-i\frac{\omega_0 t}{2}\sigma_z} = \sigma_+ e^{+i\omega_0 t}$ and $e^{+i\frac{\omega_0 t}{2}\sigma_z} \sigma_- e^{-i\frac{\omega_0 t}{2}\sigma_z} = \sigma_- e^{-i\omega_0 t}$,

$$V_I(t) = \hbar\Omega \cos(\omega_d t + \phi) (\sigma_+ e^{+i\omega_0 t} + \sigma_- e^{-i\omega_0 t}). \quad (4)$$

Now expand $\cos(\omega_d t + \phi) = \frac{1}{2}(e^{+i(\omega_d t + \phi)} + e^{-i(\omega_d t + \phi)})$ and collect terms:

$$V_I(t) = \frac{\hbar\Omega}{2} [\sigma_+ e^{+i(\omega_0 - \omega_d)t} e^{-i\phi} + \sigma_- e^{-i(\omega_0 - \omega_d)t} e^{+i\phi} + \sigma_+ e^{+i(\omega_0 + \omega_d)t} e^{+i\phi} + \sigma_- e^{-i(\omega_0 + \omega_d)t} e^{-i\phi}]. \quad (5)$$

Define the detuning $\Delta \equiv \omega_0 - \omega_d$. Then eq. (5) has two “slow” terms oscillating at Δ and two “fast” terms oscillating at $\omega_0 + \omega_d$.

3.2.3 The approximation step, made explicit

The RWA keeps the slowly varying terms and drops the rapidly varying terms:

$$V_I^{\text{RWA}}(t) = \frac{\hbar\Omega}{2} [\sigma_+ e^{+i\Delta t} e^{-i\phi} + \sigma_- e^{-i\Delta t} e^{+i\phi}]. \quad (6)$$

A compact way to see why this is controlled is to bound the first Magnus term for the discarded part. Write

$$V_I(t) = V_{I,\text{slow}}(t) + V_{I,\text{fast}}(t), \quad V_{I,\text{fast}}(t) = \frac{\hbar\Omega}{2} [\sigma_+ e^{+i(\omega_0+\omega_d)t} e^{+i\phi} + \sigma_- e^{-i(\omega_0+\omega_d)t} e^{-i\phi}]. \quad (7)$$

Then the size of its time integral is bounded by

$$\begin{aligned} \left\| \int_0^T V_{I,\text{fast}}(t) dt \right\| &\leq \frac{\hbar\Omega}{2} \left(\|\sigma_+\| \left| \int_0^T e^{+i(\omega_0+\omega_d)t} dt \right| + \|\sigma_-\| \left| \int_0^T e^{-i(\omega_0+\omega_d)t} dt \right| \right) \\ &\leq \frac{\hbar\Omega}{2} (\|\sigma_+\| + \|\sigma_-\|) \frac{2}{\omega_0 + \omega_d}. \end{aligned} \quad (8)$$

Thus, a natural small parameter is

$$\varepsilon_{\text{RWA}} \sim \frac{\Omega}{\omega_0 + \omega_d}, \quad (9)$$

and higher-order corrections generate, among other effects, the Bloch–Siegert shift [1].

3.2.4 Leading correction: Bloch–Siegert shift (linear drive)

For a linearly polarized drive as in eq. (1), the leading frequency shift that emerges beyond the RWA is the Bloch–Siegert (BS) shift. In ordinary frequency units (Hz), a commonly used near-resonant estimate is

$$\frac{\delta_{\text{BS}}}{2\pi} \approx \frac{f_R^2}{4(f_0 + f_d)}, \quad (10)$$

where $f_R = \Omega/(2\pi)$ is the on-resonance Rabi oscillation frequency in Hz under the RWA, and $f_0 = \omega_0/(2\pi)$, $f_d = \omega_d/(2\pi)$.

3.2.5 A practical “make it exact” note

If the lab drive is made *circularly polarized* (implemented experimentally by using two quadratures with a $\pi/2$ phase shift), then the counter-rotating component can be eliminated, and the step of “dropping” it becomes unnecessary. In that restricted but important case, what is usually an approximation becomes an exact simplification, and the effective Hamiltonian in the rotating frame is time independent without invoking the RWA.

3.3 Three numerical RWA examples (with real values)

3.3.1 Example RWA-1: superconducting qubit driven at 5.000 GHz

We model a superconducting circuit qubit (SCQ) as a two-level system. Choose

$$f_0 = 5.000 \text{ GHz}, \quad f_d = 5.000 \text{ GHz}, \quad f_R = \frac{\Omega}{2\pi} = 20 \text{ MHz}, \quad \Delta = \omega_0 - \omega_d = 0. \quad (11)$$

The RWA small parameter is

$$\varepsilon_{\text{RWA}} \approx \frac{f_R}{f_0 + f_d} = \frac{20 \text{ MHz}}{10.000 \text{ GHz}} = 2.0 \times 10^{-3}. \quad (12)$$

The BS shift estimate eq. (10) gives

$$\frac{\delta_{\text{BS}}}{2\pi} \approx \frac{(20 \text{ MHz})^2}{4(10.000 \text{ GHz})} = 10.0 \text{ kHz}. \quad (13)$$

On resonance, a π pulse occurs at $t_\pi = \pi/\Omega = 1/(2f_R)$:

$$t_\pi = \frac{1}{2f_R} = \frac{1}{2 \cdot 20 \text{ MHz}} = 25.0 \text{ ns}. \quad (14)$$

Because $\delta_{\text{BS}}/(2\pi)$ is 10 kHz while f_R is 20 MHz, the BS correction is comparatively tiny for this parameter set. For stronger driving, or lower carrier frequency, that separation erodes.

3.3.2 Example RWA-2: proton NMR at 3.0 T with a weak RF field

For a proton, $\gamma/(2\pi) \approx 42.57747892 \text{ MHz T}^{-1}$. With $B_0 = 3.0 \text{ T}$,

$$f_0 = \frac{\gamma}{2\pi} B_0 = 127.73243676 \text{ MHz}. \quad (15)$$

Drive slightly above resonance:

$$f_d = f_0 + 500 \text{ Hz} \Rightarrow \frac{\Delta}{2\pi} = f_0 - f_d = -500 \text{ Hz}. \quad (16)$$

Let the lab transverse RF field be linearly polarized with amplitude $B_1 = 100 \mu\text{T}$. Under the usual linear-to-circular decomposition, the co-rotating component has half amplitude, so the RWA Rabi frequency is

$$f_R = \frac{\Omega}{2\pi} = \frac{1}{2} \frac{\gamma}{2\pi} B_1 = \frac{1}{2} (42.57747892 \text{ MHz T}^{-1}) (100 \mu\text{T}) = 2128.873946 \text{ Hz}. \quad (17)$$

The fast-scale separation is extreme:

$$\varepsilon_{\text{RWA}} \approx \frac{f_R}{f_0 + f_d} \approx 8.333317 \times 10^{-6}. \quad (18)$$

The BS shift estimate yields

$$\frac{\delta_{\text{BS}}}{2\pi} \approx 4.435145 \times 10^{-3} \text{ Hz}. \quad (19)$$

Under the RWA, the generalized Rabi oscillation frequency is

$$f_{\text{eff}} = \sqrt{f_R^2 + (f_0 - f_d)^2} = \sqrt{(2128.873946 \text{ Hz})^2 + (500 \text{ Hz})^2} = 2186.802295 \text{ Hz}. \quad (20)$$

The first maximum excitation occurs at $t_{\max} = 1/(2f_{\text{eff}})$:

$$t_{\max} = 2.2864435487148223 \times 10^{-4} \text{ s} = 228.6443549 \mu\text{s}. \quad (21)$$

The maximum excitation probability is reduced by detuning:

$$P_{e,\max} = \frac{f_R^2}{f_{\text{eff}}^2} = 0.9477217589854038. \quad (22)$$

This off-resonant effect is slow and experimentally visible, while the counter-rotating corrections remain minuscule.

3.3.3 Example RWA-3: optical transition near 384.230 THz

Consider an optical transition with

$$f_0 = 384.230 \text{ THz}, \quad f_d = f_0 + 0.5 \text{ MHz}, \quad \Rightarrow \quad \frac{\Delta}{2\pi} = f_0 - f_d = -0.5 \text{ MHz}. \quad (23)$$

Let the RWA Rabi frequency be $f_R = \Omega/(2\pi) = 5 \text{ MHz}$. Then

$$\varepsilon_{\text{RWA}} \approx \frac{f_R}{f_0 + f_d} \approx 6.506519528338157 \times 10^{-9}. \quad (24)$$

The BS estimate is

$$\frac{\delta_{\text{BS}}}{2\pi} \approx 8.133149410422697 \times 10^{-3} \text{ Hz}. \quad (25)$$

The effective oscillation frequency and the time to first maximum are

$$f_{\text{eff}} = \sqrt{(5 \text{ MHz})^2 + (0.5 \text{ MHz})^2} = 5.02493781056 \text{ MHz}, \quad t_{\text{max}} = \frac{1}{2f_{\text{eff}}} = 9.950371902099891 \times 10^{-8} \text{ s}. \quad (26)$$

The detuning-limited maximum excitation is

$$P_{e,\text{max}} = \frac{f_R^2}{f_{\text{eff}}^2} = 0.9900990099009901. \quad (27)$$

Here, the RWA is extraordinarily accurate, and the dominant experimental limitations typically come from decoherence, laser noise, or multilevel structure, not from counter-rotating physics.

3.3.4 RWA examples summary table

Table 3: Summary of the three RWA numerical examples. Note: $\varepsilon_{\text{RWA}} \approx f_R/(f_0 + f_d)$ and $\Delta = 2\pi(f_0 - f_d)$.

Example	f_0 (Hz)	Drive scheme (f_d)	f_R (Hz)	$\Delta/2\pi$ (Hz)	ε_{RWA}	$\delta_{\text{BS}}/2\pi$ (Hz)
RWA-1 (SCQ)	5.0000e9	$f_d = f_0$	2.0000e7	0.0000	2.0000e-3	1.0000e4
RWA-2 (NMR)	1.2773e8	$f_d = f_0 + 500.0000 \text{ Hz}$	2.1289e3	-5.0000e2	8.3333e-6	4.4351e-3
RWA-3 (Optical)	3.8423e14	$f_d = f_0 + 0.5000 \text{ MHz}$	5.0000e6	-5.0000e5	6.5065e-9	8.1331e-3

4 Rotating frame approximation (RFA)

4.1 Intuitive explanation

If you record a spinning fan with a camera that spins at almost the same rate, then, relative to the camera, the fan looks like it is turning slowly, and you can measure its shape and motion more easily. In quantum driving, a rotating frame is that spinning camera. The rotating frame transformation is exact, but, once transformed, leftover terms can oscillate at about twice the carrier frequency. The rotating frame approximation (RFA) is the controlled act of dropping those twice-the-carrier terms, because, over the slow dynamics you care about, they mostly cancel.

4.2 Graduate level derivation: explicit rotating frame transformation, then the approximation step

4.2.1 Exact rotating frame transformation (RFT)

Start again from eq. (1). Define the rotating frame state

$$|\psi_{\text{rot}}(t)\rangle = U^\dagger(t) |\psi(t)\rangle, \quad U(t) = \exp\left(-i\frac{\omega_{\text{ref}} t}{2} \sigma_z\right), \quad (28)$$

where ω_{ref} is the chosen reference rotation rate (often $\omega_{\text{ref}} = \omega_d$). The transformed Schrödinger equation is

$$i\hbar \frac{d}{dt} |\psi_{\text{rot}}(t)\rangle = H_{\text{rot}}(t) |\psi_{\text{rot}}(t)\rangle, \quad H_{\text{rot}}(t) = U^\dagger H U - i\hbar U^\dagger \dot{U}. \quad (29)$$

Since $\dot{U} = -i\frac{\omega_{\text{ref}}}{2} \sigma_z U$, we get

$$-i\hbar U^\dagger \dot{U} = \frac{\hbar \omega_{\text{ref}}}{2} \sigma_z. \quad (30)$$

Also, $U^\dagger \sigma_z U = \sigma_z$, and the transverse operator rotates:

$$U^\dagger \sigma_x U = \sigma_x \cos(\omega_{\text{ref}} t) + \sigma_y \sin(\omega_{\text{ref}} t). \quad (31)$$

Insert eq. (31) into eq. (29):

$$H_{\text{rot}}(t) = \frac{\hbar(\omega_0 - \omega_{\text{ref}})}{2} \sigma_z + \hbar \Omega \cos(\omega_d t + \phi) [\sigma_x \cos(\omega_{\text{ref}} t) + \sigma_y \sin(\omega_{\text{ref}} t)]. \quad (32)$$

4.2.2 Choosing the reference rate and isolating $2\omega_d$ terms

Set $\omega_{\text{ref}} = \omega_d$ (the standard co-rotating choice). Then, using trig identities,

$$\cos(\omega_d t + \phi) \cos(\omega_d t) = \frac{1}{2} [\cos \phi + \cos(2\omega_d t + \phi)], \quad (33)$$

$$\cos(\omega_d t + \phi) \sin(\omega_d t) = \frac{1}{2} [\sin \phi + \sin(2\omega_d t + \phi)], \quad (34)$$

so eq. (32) becomes

$$\begin{aligned} H_{\text{rot}}(t) &= \frac{\hbar \Delta}{2} \sigma_z + \frac{\hbar \Omega}{2} (\cos \phi \sigma_x + \sin \phi \sigma_y) \\ &\quad + \frac{\hbar \Omega}{2} (\cos(2\omega_d t + \phi) \sigma_x + \sin(2\omega_d t + \phi) \sigma_y). \end{aligned} \quad (35)$$

The last line oscillates at $2\omega_d$.

4.2.3 Rotating frame approximation (RFA)

The rotating frame approximation drops the explicitly fast $2\omega_d$ terms in eq. (35), producing a time-independent effective Hamiltonian

$$H_{\text{rot}}^{(\text{RFA})} = \frac{\hbar\Delta}{2}\sigma_z + \frac{\hbar\Omega}{2}(\cos\phi\sigma_x + \sin\phi\sigma_y). \quad (36)$$

As in the RWA derivation, a natural control parameter is $\Omega/(2\omega_d)$ (or, in Hz, $f_R/(2f_d)$), and the leading corrections include the Bloch–Siegert shift [1]. Put differently, for the basic two-level drive model, the RWA and the RFA are mathematically equivalent approximations expressed in two complementary languages: interaction-picture frequency selection versus rotating-frame averaging.

4.2.4 Time-dependent phase or frequency (why rotating frames keep paying off)

If the drive is written with an explicit time-dependent phase $\phi(t)$, then $\cos(\omega_dt + \phi(t))$ can be viewed as a carrier with a slowly varying phase. In an *instantaneous* rotating frame (using $U(t) = \exp[-i(\omega_dt + \phi(t))\sigma_z/2]$), an extra term proportional to $\dot{\phi}(t)\sigma_z$ appears, so phase ramps become effective detunings. This is why, in contemporary qubit control, *virtual Z rotations* can be implemented by phase updates: a rotating-frame viewpoint makes them algebraically transparent.

4.3 Three numerical rotating frame approximation examples (with real values)

4.3.1 Example RFA-1: resonant single-qubit X and Y gates by phase choice

Choose a superconducting qubit with

$$f_0 = 5.000 \text{ GHz}, \quad f_d = 5.000 \text{ GHz} \quad (\Delta = 0), \quad f_R = \frac{\Omega}{2\pi} = 20 \text{ MHz}. \quad (37)$$

Then eq. (36) gives

$$H_{\text{rot}}^{(\text{RFA})} = \frac{\hbar\Omega}{2}(\cos\phi\sigma_x + \sin\phi\sigma_y). \quad (38)$$

Two phase choices implement orthogonal rotation axes:

$$\phi = 0 \Rightarrow H = \frac{\hbar\Omega}{2}\sigma_x \quad (\text{an } X \text{ rotation}), \quad (39)$$

$$\phi = \frac{\pi}{2} \Rightarrow H = \frac{\hbar\Omega}{2}\sigma_y \quad (\text{a } Y \text{ rotation}). \quad (40)$$

The gate times follow directly. A $\pi/2$ pulse duration is

$$t_{\pi/2} = \frac{\pi/2}{\Omega} = \frac{1}{4f_R} = 12.5 \text{ ns}, \quad (41)$$

and a π pulse duration is

$$t_\pi = \frac{\pi}{\Omega} = \frac{1}{2f_R} = 25.0 \text{ ns}. \quad (42)$$

Here, the rotating frame approximation turns a lab-frame oscillatory drive into a static effective control Hamiltonian whose axis is set by phase.

4.3.2 Example RFA-2: off-resonant MRI-like scenario, effective field tilt in the rotating frame

Take proton magnetic resonance at $B_0 = 1.5$ T:

$$f_0 = \frac{\gamma}{2\pi} B_0 = (42.57747892 \text{ MHz T}^{-1})(1.5 \text{ T}) = 63.86621838 \text{ MHz}. \quad (43)$$

Drive slightly below resonance:

$$f_d = f_0 - 2.0 \text{ kHz} \Rightarrow \frac{\Delta}{2\pi} = f_0 - f_d = +2.0 \text{ kHz}. \quad (44)$$

Let the RWA Rabi frequency be $f_R = \Omega/(2\pi) = 1.0$ kHz and choose $\phi = 0$ for an σ_x control quadrature. Then

$$H_{\text{rot}}^{(\text{RFA})} = \frac{\hbar}{2} (\Delta \sigma_z + \Omega \sigma_x). \quad (45)$$

The effective precession frequency (in Hz) is

$$f_{\text{eff}} = \sqrt{f_R^2 + \left(\frac{\Delta}{2\pi}\right)^2} = \sqrt{(1.0 \text{ kHz})^2 + (2.0 \text{ kHz})^2} = 2.236067977 \text{ kHz}. \quad (46)$$

The effective field tilt angle away from $+z$ toward $+x$ is

$$\theta = \arctan\left(\frac{f_R}{\Delta/2\pi}\right) = \arctan\left(\frac{1}{2}\right) = 26.56505118^\circ. \quad (47)$$

Starting in the ground state, the maximum excitation probability is reduced:

$$P_{e,\text{max}} = \frac{f_R^2}{f_{\text{eff}}^2} = 0.2. \quad (48)$$

The time to the first maximum is

$$t_{\text{max}} = \frac{1}{2f_{\text{eff}}} = 2.2360679774997895 \times 10^{-4} \text{ s} = 223.6067977 \mu\text{s}. \quad (49)$$

This is the classic rotating-frame picture: magnetization (or the Bloch vector) precesses about a static *effective field* tilted by detuning.

4.3.3 Example RFA-3: chirped drive (adiabatic rapid passage) and a Landau–Zener estimate

Let a qubit have $f_0 = 5.000$ GHz, and use an *instantaneous* rotating frame so the effective Hamiltonian is

$$H_{\text{rot}}(t) = \frac{\hbar}{2} (\Delta(t) \sigma_z + \Omega \sigma_x), \quad (50)$$

where $\Delta(t) = \omega_0 - \omega_d(t)$ is a controlled sweep. Choose:

$$f_R = \frac{\Omega}{2\pi} = 2.0 \text{ MHz}, \quad \frac{\Delta(t)}{2\pi} \text{ sweeps linearly from } -20 \text{ MHz to } +20 \text{ MHz in } T = 10 \mu\text{s}. \quad (51)$$

The detuning sweep rate in Hz/s is

$$\Delta f_{\text{span}} \equiv (+20 \text{ MHz} - (-20 \text{ MHz})) = 40 \text{ MHz}, \quad (52)$$

$$\alpha_{\text{Hz}} \equiv \left| \frac{d}{dt} \left(\frac{\Delta(t)}{2\pi} \right) \right| = \frac{\Delta f_{\text{span}}}{T} = \frac{40 \text{ MHz}}{10 \mu\text{s}} = 4.0 \times 10^{12} \text{ Hz s}^{-1}. \quad (53)$$

For the standard Landau–Zener (LZ) avoided-crossing model [2], applied to the rotating-frame Hamiltonian $H_{\text{rot}}(t) = \frac{\hbar}{2}(\Delta(t)\sigma_z + \Omega\sigma_x)$ with a *locally linear* sweep through the crossing, $\Delta(t) \approx \dot{\Delta}t$ near $\Delta = 0$, the diabatic (i.e. non-adiabatic) transition probability can be written as

$$P_{\text{nonad}} \equiv P_{\text{LZ}} \approx \exp\left(-\frac{\pi\Omega^2}{2|\dot{\Delta}|}\right). \quad (54)$$

Here P_{nonad} is the probability to *fail* to follow the instantaneous adiabatic eigenstate across the avoided crossing; correspondingly, $P_{\text{ad}} \approx 1 - P_{\text{nonad}}$ is the adiabatic-following probability.

To express eq. (54) using frequency (Hz) quantities, define $f_R \equiv \Omega/(2\pi)$ and the detuning sweep rate

$$\alpha_{\text{Hz}} \equiv \frac{d}{dt}\left(\frac{\Delta}{2\pi}\right) = \frac{1}{2\pi}\dot{\Delta}, \quad (55)$$

so that $\dot{\Delta} = 2\pi\alpha_{\text{Hz}}$. Then eq. (54) is equivalently

$$P_{\text{nonad}} \approx \exp\left(-\frac{\pi^2 f_R^2}{\alpha_{\text{Hz}}}\right), \quad (56)$$

which is dimensionless and directly matches the quantities computed in this example.

Strictly, the canonical or textbook version of the LZ result assumes an effectively infinite sweep ($t : -\infty \rightarrow +\infty$). A finite-span sweep is well-approximated by eq. (56) provided the endpoints are far from the avoided crossing, i.e. $|\Delta(t_i)|, |\Delta(t_f)| \gg \Omega$, or equivalently $|\Delta|/(2\pi) \gg f_R$. Here the endpoints satisfy $|\Delta|/(2\pi) = 20 \text{ MHz} = 10 f_R$, which is typically adequate; increasing the span improves agreement further if desired.

Insert the numbers:

$$P_{\text{nonad}} \approx \exp\left(-\frac{\pi^2(2.0 \text{ MHz})^2}{4.0 \times 10^{12} \text{ Hz s}^{-1}}\right) = \exp(-\pi^2) = 5.172318620381234 \times 10^{-5}. \quad (57)$$

A related adiabaticity indicator (in angular units) is

$$Q \equiv \frac{\Omega^2}{|\dot{\Delta}|} = \frac{2\pi f_R^2}{\alpha_{\text{Hz}}}, \quad P_{\text{nonad}} \approx \exp\left(-\frac{\pi}{2}Q\right), \quad (58)$$

which is comfortably larger than 1 here, consistent with a strongly adiabatic sweep.

4.3.4 RFA examples summary table

Table 4: Summary of the three rotating frame approximation numerical examples.

Example	f_0 (Hz)	Drive scheme (f_d)	f_R (Hz)	$\Delta/2\pi$ (Hz)	Key computed outcome
RFA-1 (SCQ gates)	5.0000e9	$f_d = f_0$	2.0000e7	0.0000	$t_{\pi/2} = 12.5000 \text{ ns}$, $t_\pi = 25.0000 \text{ ns}$
RFA-2 (MRI-like)	6.3866e7	$f_d = f_0 - 2.0000 \text{ kHz}$	1.0000e3	2.0000e3	$f_{\text{eff}} = 2.2360 \text{ kHz}$, $\theta = 26.6000^\circ$, $P_{e,\text{max}} = 0.2000$
RFA-3 (Chirped)	5.0000e9	$\Delta(t)/(2\pi) : -20.0000 \text{ MHz} \rightarrow +20.0000 \text{ MHz}$ in 10.0000 ps	2.0000e6	time-dependent	$\alpha = 4.0000e12 \text{ Hz s}^{-1}$, $P_{\text{nonad}} \approx 5.1700e-5$

5 Context, lineage, and “where to go next”

Historically, the rotating-field viewpoint appears early in magnetic resonance and in I. I. Rabi’s molecular-beam work [3], while the explicit counter-rotating correction that now carries Bloch and Siegert’s names appears in [1]. For periodically driven systems, Floquet methods [4] give an exact framework in which the RWA and rotating-frame averaging can be understood as approximations that keep only selected Fourier blocks. In modern strong-driving settings, where Ω is no longer small compared with ω_0 , the quantum Rabi model and its exact structures become relevant [5].

References

- [1] F. Bloch and A. Siegert, “Magnetic resonance for nonrotating fields,” *Physical Review*, vol. 57, pp. 522–527, 1940. DOI: [10.1103/PhysRev.57.522](https://doi.org/10.1103/PhysRev.57.522).
- [2] S. N. Shevchenko, S. Ashhab, and F. Nori, “Landau–zener–stückelberg interferometry,” *Physics Reports*, vol. 492, no. 1, pp. 1–30, 2010. DOI: [10.1016/j.physrep.2010.03.002](https://doi.org/10.1016/j.physrep.2010.03.002). arXiv: [0911.1917 \[quant-ph\]](https://arxiv.org/abs/0911.1917).
- [3] I. I. Rabi, “Space quantization in a gyrating magnetic field,” *Physical Review*, vol. 51, pp. 652–654, 1937. DOI: [10.1103/PhysRev.51.652](https://doi.org/10.1103/PhysRev.51.652).
- [4] J. H. Shirley, “Solution of the schrödinger equation with a hamiltonian periodic in time,” *Physical Review*, vol. 138, B979–B987, 1965. DOI: [10.1103/PhysRev.138.B979](https://doi.org/10.1103/PhysRev.138.B979).
- [5] D. Braak, “Integrability of the rabi model,” *Physical Review Letters*, vol. 107, p. 100401, 2011. DOI: [10.1103/PhysRevLett.107.100401](https://doi.org/10.1103/PhysRevLett.107.100401). arXiv: [1103.2461 \[math-ph\]](https://arxiv.org/abs/1103.2461).